Microsystem Technologies (2020) 26:1881–1888
https://doi.org/10.1007/s00542-019-04737-0

TECHNICAL PAPER

A compact broadband GFET based rectenna for RF energy harvesting applications

Neeta Singh[1] · Sachin Kumar[2] · Binod Kumar Kanaujia[3] · Mirza Tariq Beg[1] · Mainuddin[1] · Sandeep Kumar[4]

Received: 3 December 2019 / Accepted: 21 December 2019 / Published online: 2 January 2020

Abstract

In this paper, a compact GFET-based rectifier integrated with a monopole antenna is proposed for wireless energy harvesting applications. The GFET increases impedance bandwidth of the rectifying circuit, thus covering a range of 22.5–27.5 GHz. The sensing antenna is a triangular monopole with truncated corners for realizing circular polarization at the frequencies 24.25 GHz and 27 GHz. By the help of $\lambda/4$ transformer, the sensing antenna is matched with the proposed GFET rectifier. The RF-DC conversion efficiency realized is 80% at 5 dBm for the load of 5 KΩ, and the output DC voltage observed is 6.8 V. The modified ground plane triangular monopole antenna shows a peak gain of 7.8 dBi. The designed rectenna prototype is fabricated and found simulated and measured results are in good agreement.

1 Introduction

With the expansion of wireless operating devices/systems, there is an increase in ambient RF energy available in the environment (Valenta and Durgin 2014). This energy can be collected from the surroundings and consumed for low power electrical and electronic components in wireless sensor networks (WSN), machine to machine (M2M) communication and internet of things (IoT) based sensors. For the process of wireless power transfer (WPT)/wireless energy harvesting (WEH), a rectifying antenna arrangement commonly known as "wireless battery" or rectenna is usually used (Jabbar et al. 2010; Georgiou et al. 2016; Mimis et al. 2015). The rectenna consists of a sensing antenna, AC–DC rectifier, matching network and a DC pass filter (Singh et al. 2018a, b; Cui et al. 2014). The energy harvesting methods offer a considerable solution for battery recharging or replacement. Rectenna structures can be used for recharging batteries in the contemporary sensor systems installed at smart houses, wearable/implanted medical devices, environmental monitoring, and automotive applications. As a result, these sensors are expected to connect/communicate with the IoT systems and function autonomously for years. In the case of WPT/WEH, the sensing antenna does not have information about the direction of the received power. Therefore, the basic goal is to enhance the probability of reception by proposing sensing antennas with high gain, broadband or multiband characteristics, and polarization diversity. In the last few years, for the efficient operation of the rectenna, a variety of multiple and wideband antennas have been reported (Sun et al. 2012; Georgiadis et al. 2010; Song et al. 2015; Sun et al. 2013; Yang et al. 2018; Chandravanshi et al. 2018). Most of the reported antennas resonate for ISM, GSM, UMTS, WLAN, and WiMAX application bands. A high-efficiency rectenna with planar high gain antenna operating at 2.45 GHz ISM band was presented in Sun et al. (2012); rectenna based on dual linearly polarized aperture coupled square patch antenna in Georgiadis et al. (2010); dipole antenna with dual polarization and harmonic suppression characteristic was reported in Song et al. (2015); a high gain dual band antenna operating for GSM and UMTS applications in Sun et al. (2013); compact rectenna based on circularly polarized wide slot antenna

✉ Sachin Kumar
gupta.sachin0708@gmail.com

[1] Department of Electronics and Communication Engineering, Jamia Millia Islamia, New Delhi 110025, India

[2] School of Electronics Engineering, Kyungpook National University, Daegu 41566, Republic of Korea

[3] School of Computational and Integrative Sciences, Jawaharlal Nehru University, New Delhi 110067, India

[4] Department of Electronics and Communication Engineering, National Institute of Technology Karnataka, Surathkal, Mangalore 575025, India

operating at 5.8 GHz was proposed in Yang et al. (2018). A differentially-fed triple band rectenna using Villard voltage doubler and operating for UMTS, WLAN, and WiMAX bands was reported in Chandravanshi et al. (2018).

But a very few rectenna have been reported for energy harvesting in high-frequency bands. A rectenna comprised of four cross dipole antenna arrays and a Schottky diode was designed for K and Ka operating bands (Okba et al. 2017). In Yoo and Chang (1992), a dual band rectenna was proposed with a conversion efficiency of 60% and 39% at frequencies 10 GHz and 35 GHz, respectively. Several millimeter-wave based rectenna configurations with optimal RF to DC conversion efficiency at 24 GHz were presented (Shinohara et al. 2011; Collado and Georgiadis 2013; Ladan et al. 2014), these structures were based on substrate integrated waveguide (SIW) cavity-backed technique. Various types of planar monopole antennas have also been reported for RF energy harvesting. A printed monopole antenna based rectenna has a large operating range, compact size, light weight, and easy integration capability (Monti et al. 2012a, b). However, most of the reported rectenna designs make use of single, double, or narrowband antennas and Schottky diodes for the rectification of RF signals. Since the incident power available from electromagnetic (EM) signals is too small for a Schottky diode to operate in the rectenna circuitry, therefore setting a limit on practicability (Zhang et al. 2018; Li and Li 2004). Also, the reported rectenna designs have a larger size and complex antenna geometry, thus, making them difficult to fabricate and integrate with small portable terminals. Hence, there is a need for compact high gain circularly polarized wideband antenna and a rectifier with high conversion efficiency to sense EM signals from all directions without facing the complications of antenna orientation and multipath fading effects.

In this paper, a circularly polarized graphene field effect transistor (GFET)-based rectenna integrated with a monopole antenna is designed for sensing high-frequency RF signals. The proposed equilateral triangular-shaped broadband monopole antenna consists of truncated corners, and an asymmetric cross slot, embedded in the center of the radiator for realizing circular polarization. Compared to square, circular or rectangular geometry, the equilateral triangular patch antenna has the advantage of compact size. The RF to DC conversion efficiency of the proposed rectenna is 80% at 5 dBm for the load of 5 KΩ. The simulations related to the graphene FET rectifier are carried out using Keysight ADS® (Keysight Technologies 2015) and the antenna simulations were performed in Ansys HFSS® (Ansys Corporation 2014).

2 Antenna design

The top and side views of the proposed equilateral triangular ring-shaped sensing antenna are shown in Fig. 1a, b, respectively. The antenna is comprised of a modified rectangular ground plane and a triangular radiating patch excited through a microstrip feed line of 50 Ω. By means of loading, an equilateral triangle is introduced in the center of the triangular ring for enhancing the impedance bandwidth. To realize circular polarization, the antenna corners are truncated by a quadrant, for generating a pair of orthogonal modes of nearly equal amplitude and quadrature phase difference. Further, an asymmetrical cross slot is loaded in the center of the proposed antenna for exciting another circularly polarized band. The antenna is fabricated on low cost FR-4 substrate of dielectric constant 4.4 and thickness 1.6 mm. The overall dimension of the proposed antenna is 40 × 40 × 1.6 mm^3. The optimized dimensions of the designed antenna are specified in Table 1.

The designing steps of the proposed antenna are illustrated in Fig. 2. The antenna shown in Fig. 2a (step-1) is a simple triangular shape radiator with a modified rectangular ground plane and fed through microstrip line feed. The antenna shows wideband performance with a resonating frequency centered around 24 GHz. Next, in step-2, a triangular slot is etched from the center of the radiator, thus forming a triangular ring-shaped structure, as illustrated in Fig. 2b. As most of the current exist on the edges only, the resonating behaviour of the triangular ring-shaped antenna is almost similar to the antenna of step-1. Further, for enhancing the impedance bandwidth of the antenna, an equilateral triangle is introduced in the center of the triangular ring by means of loading (step-3), as shown in

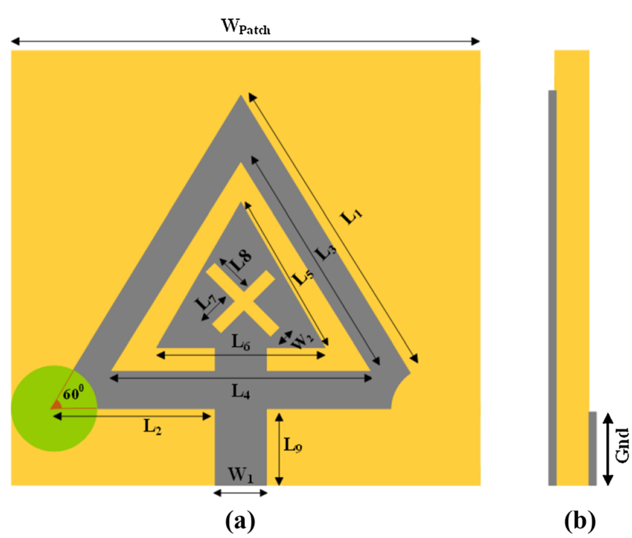

Fig. 1 Schematic of the proposed monopole antenna **a** top view, **b** side view

Table 1 Dimension of the proposed monopole antenna

Parameter	Value (mm)	Parameter	Value (mm)
W_{Patch}	40	Gnd	5.25
L_9	6	W_1	3
L_1	34	L_2	17.5
L_3	25	L_4	25
L_5	16	L_6	16
L_7	3	L_8	4
W_2	1	R	4.5

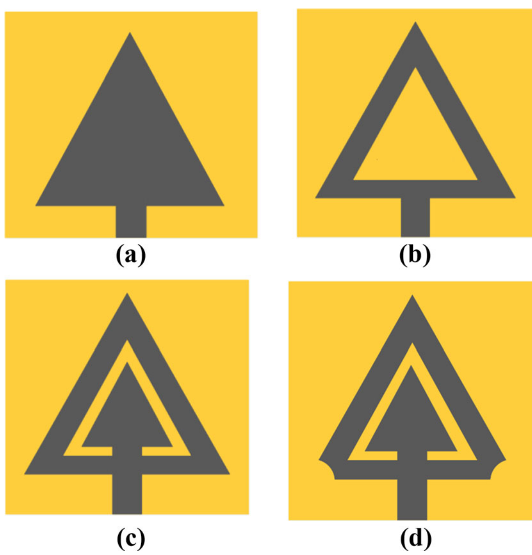

Fig. 2 Evolution steps of the proposed antenna **a** step-1, **b** step-2, **c** step-3, **d** step-4

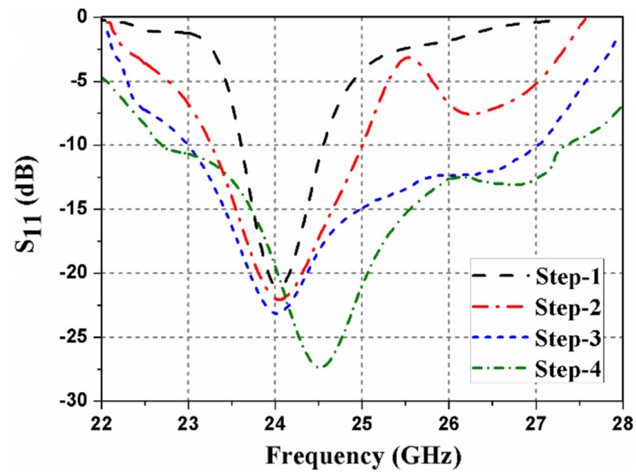

Fig. 3 Reflection coefficient characteristics of the antenna designing steps

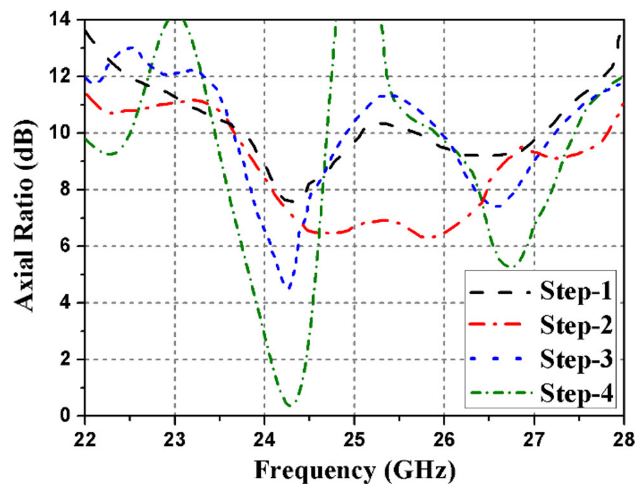

Fig. 4 Axial ratio response of the antenna designing steps

Fig. 2c. The antennas designed in steps-1 to -3 are linearly polarized structures. In the subsequent step, the corners of the proposed equilateral triangle are truncated by means of the quarter part of a circle (Fig. 2d), to introduce two orthogonal modes of nearly equal amplitude and 90° phase difference for realizing circular polarization, the radius of the circle is $R = 4.5$ mm.

In the last step, as shown in Fig. 1a, an asymmetrical cross slot is loaded in the center of the triangular patch for realizing another circularly polarized band within the antenna resonating range. The corner truncation and loading of a cross slot in the radiator change the resonating frequency band of the antenna to a lower region, thus improving the -10 dB impedance bandwidth of the antenna. In addition to this, a significant improvement in the 3-dB axial ratio band is seen. The reflection coefficients and axial ratio comparison of antenna designing steps are represented in Figs. 3 and 4, respectively.

The antenna shown in Fig. 1 is the final designed broadband monopole antenna. Figure 5a illustrates the simulated and measured reflection coefficients of the proposed antenna. It can be seen that the antenna resonates in the range of 22.5–27.5 GHz with a total bandwidth of 5 GHz. The simulated and measured axial ratio curves of the proposed monopole antenna are shown in Fig. 5b and it can be noticed that the antenna radiates circularly polarized waves at the frequencies 24.25 GHz and 27 GHz. The simulated and measured gain plots of the proposed antenna are represented in Fig. 5c. A measured peak gain of around 7.8 dBi is achieved in the resonating band of the proposed antenna. The simulated surface current distributions of the proposed monopole antenna at 24 GHz, 25 GHz, and 26 GHz are shown in Fig. 6a–c, respectively. The proposed single feed antenna design has numerous advantages like fabrication simplicity, small size, easy matching, and exhibit two circularly polarized bands. Also, there is no need for any external polarizer or loading of high-

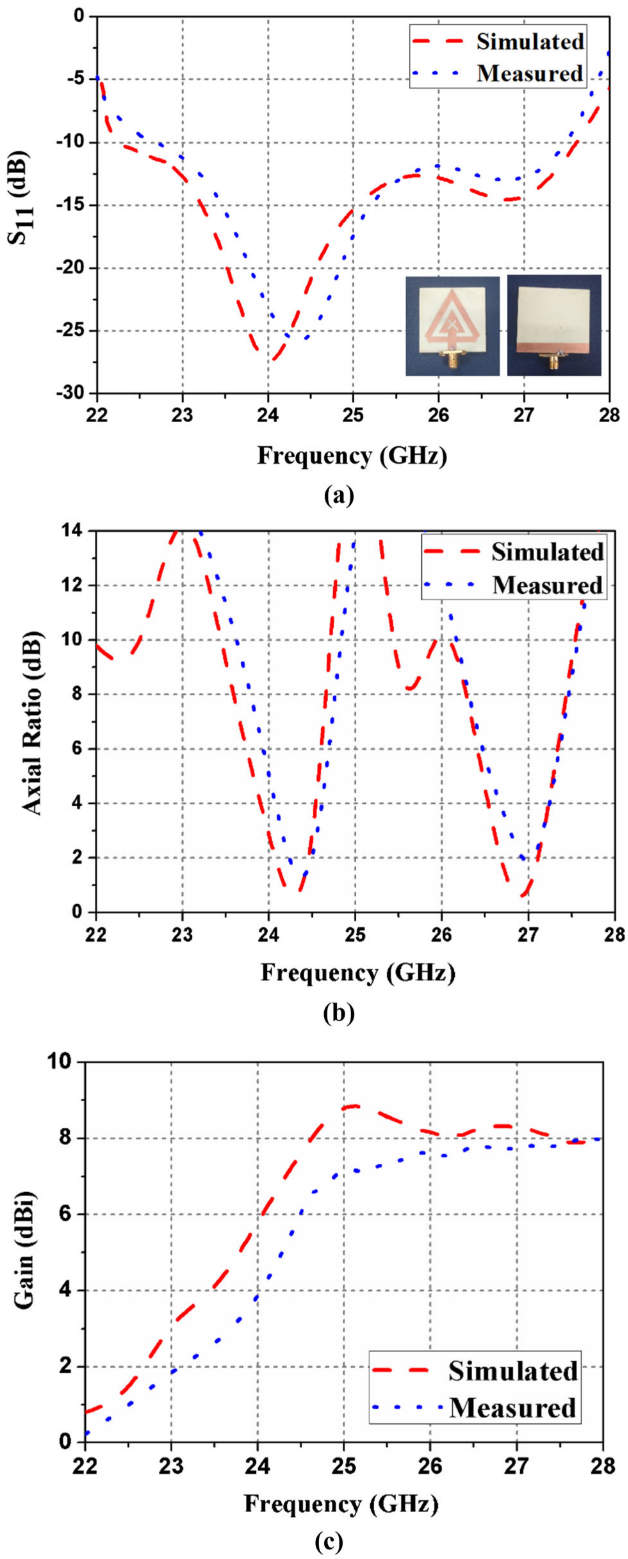

Fig. 5 Simulated and measured response of the proposed antenna **a** reflection coefficients, **b** axial ratio, **c** gain

frequency active devices for the generation of circularly polarized waves.

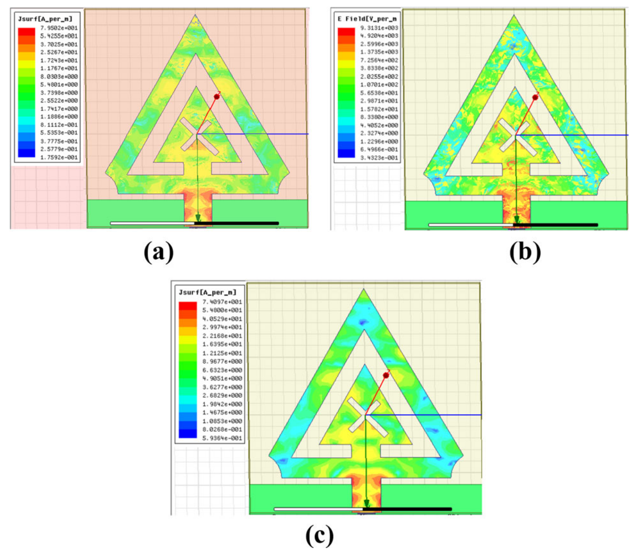

Fig. 6 Current distribution at **a** 24 GHz, **b** 25 GHz, **c** 26 GHz

3 Rectifier

By using graphene as the rectifying element, the RF energy can be harvested with high efficiency. In most of the reported works on rectenna, the rectification of RF signals is realized by using Schottky diodes or CMOS devices. But, in the case of practical rectenna, the incident power available from EM signals is too low for a Schottky diode or normal FET to operate in the rectenna circuitry. Therefore, a GFET based rectenna may be a good choice for effective RF-DC conversion. In addition to its large saturation and high band structure velocity, the proposed rectenna shows high conversion efficiency even at higher frequencies.

The cut-off frequency can be derived from (Schwierz 2010)

$$f_T = \frac{g_m}{2\pi} \frac{1}{(C_{GS}+C_{GD})[1+g_{DS}(R_S+R_D)+C_{GD}g_m(R_S+R_D)]} \quad (1)$$

where g_m is the transconductance of GFET, R_S is the source resistance, R_D is the drain resistance, C_{GS} is the gate to source capacitance and C_{GD} is the gate to drain capacitance.

$$g_m = \frac{\partial I_{DS}}{\partial V_{GS}} \quad (2)$$

$$g_{DS} = \frac{\partial I_{DS}}{\partial V_{DS}} \quad (3)$$

Figure 7a–c shows different configurations of the rectenna layout using a diode, CMOS and GFET as the rectifying element, respectively. From small signal capacitive circuit of Fig. 8a, it is clear that the cut-off frequency can

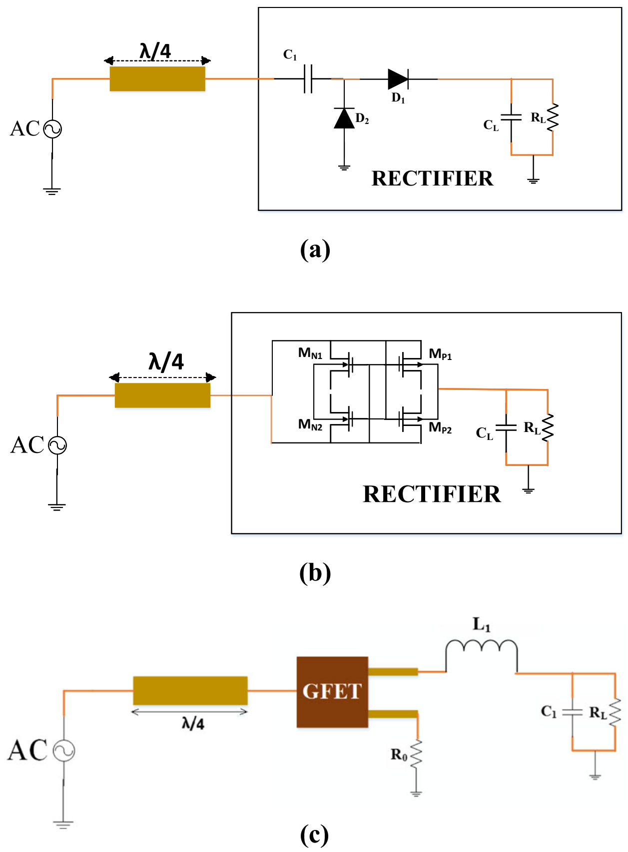

Fig. 7 Rectenna layout of **a** diode rectifier, **b** CMOS rectifier, **c** GFET rectifier

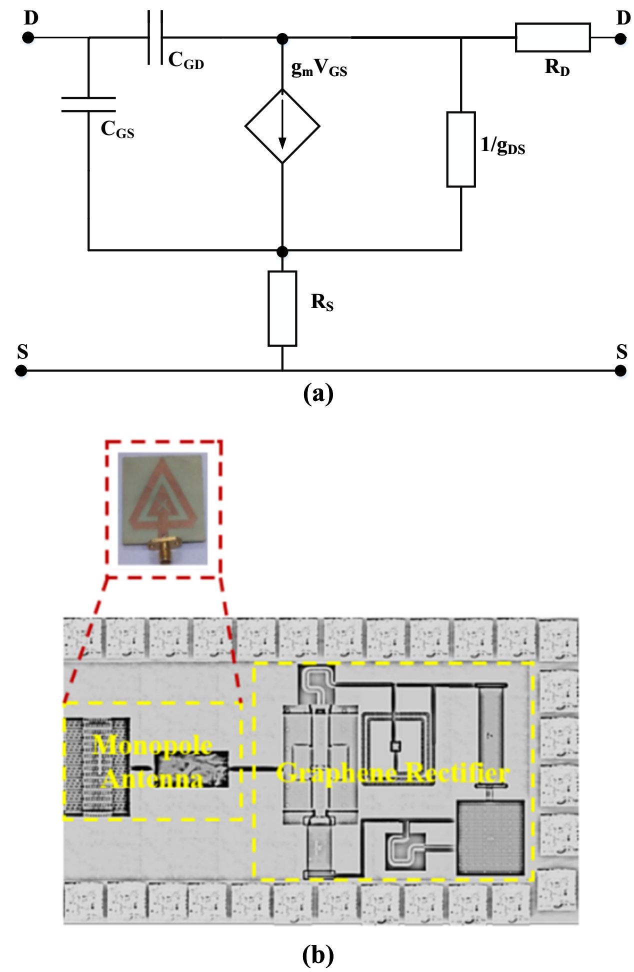

Fig. 8 Rectenna **a** small signal capacitive circuit, **b** fabricated microchip prototype

be increased by increasing the transconductance of the device. Also, it can be improved when $g_{DS} = 0$, which can be done by biasing the device into the saturation region.

The graphene is a zero band gap material also called a semi-metal and exhibits high mobility, conductivity, stability, flexibility, and transparency. The fabrication of graphene FET begins with the inclusion of an oxidation layer, by exposing the substrate in an oxidation furnace. The chemical vapour deposition process is used for growing a single layer of graphene, and during this process, the wafer of graphene is kept at a temperature of 960 °C. Using the process of thermal evaporation, the source and drain terminals are integrated within the graphene transistor. Subsequently, by the process of lithography, a gate electrode is integrated into the center of the transistor. As shown in Fig. 8b, the proposed GFET rectifier circuit is fabricated on RT/Duroid 5880 dielectric substrate.

In Fig. 9, the graphene FET, CMOS, and Schottky diode responses are compared and it is noticed that the response of graphene FET is much better compared to the Schottky and CMOS rectifying diodes. The proposed rectenna is based on graphene technology making use of a graphene FET rectifier for converting RF signals to DC power. The sensing antenna connected at the front end of the circuit

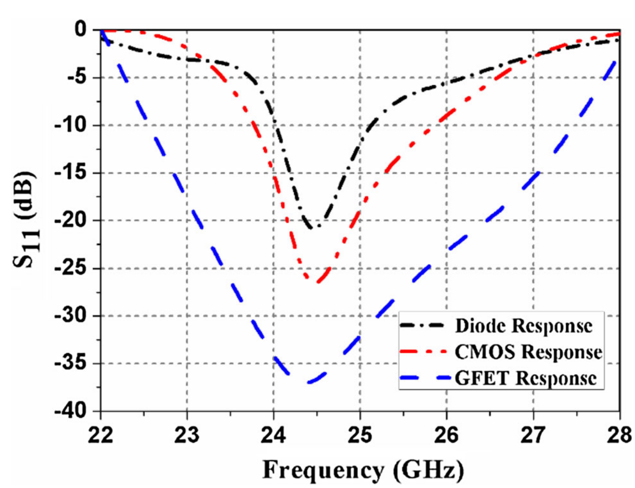

Fig. 9 Simulated return loss comparison of the Schottky, CMOS and GFET device

captures the high-frequency EM signals and passes these signals to the GFET rectifier for the purpose of rectification. For efficient energy conversion, an impedance matching element is required between the sensing antenna and the rectifying diodes. And, here in this design, the impedance matching is achieved with the help of $\lambda/4$ impedance transformer connected between the two rectenna elements as shown in Fig. 7c.

The impedance can be expressed as

$$Z_{in} = Z_1 \left[\frac{R_L + jZ_1 \tan \beta l}{Z_1 + jR_L \tan \beta l} \right] \quad (4)$$

where Z_{in} is the input impedance, Z_1 is the quarter wave impedance, $l = \lambda/4$ and $\beta = {}^{2\pi}/_{\lambda}$. Therefore,

$$Z_{in} = \frac{Z_1^2}{R_L} \quad (5)$$

$$Z_1 = \sqrt{Z_{in} \times R_L} \quad (6)$$

By this the matching is achieved for a wide frequency range.

The simulated and measured reflection coefficients of the rectenna are shown in Fig. 10. The measured and simulated results are in good agreement, which shows accuracy of the impedance matching circuit at 24 GHz. The GFET rectifier is followed by a DC pass filter which produces a smooth rectified output. At the load, a resistor of 5 KΩ is connected in shunt with the capacitor for storing the energy. The designed rectenna is compact in size and shows a good percentage of output efficiency. The transfer characteristic of graphene FET for different drain source voltage (V_{DS}) is shown in Fig. 11. It can be observed from the graph when the gate voltage is less than the Dirac voltage, the drain source current (I_{DS}) increases and saturates at a higher value of V_{GS}.

The RF to DC conversion efficiency of the rectenna is calculated as

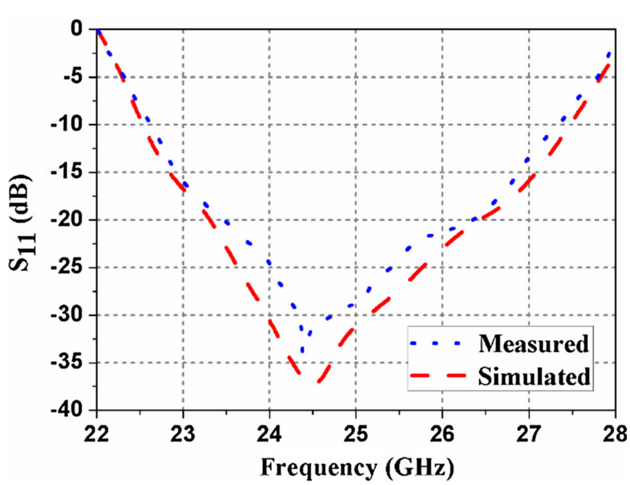

Fig. 10 Reflection coefficients of the proposed rectenna

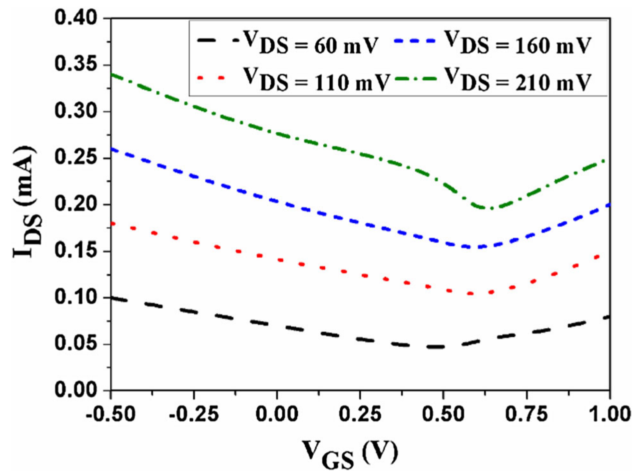

Fig. 11 Transfer characteristic of GFET for different V_{DS}

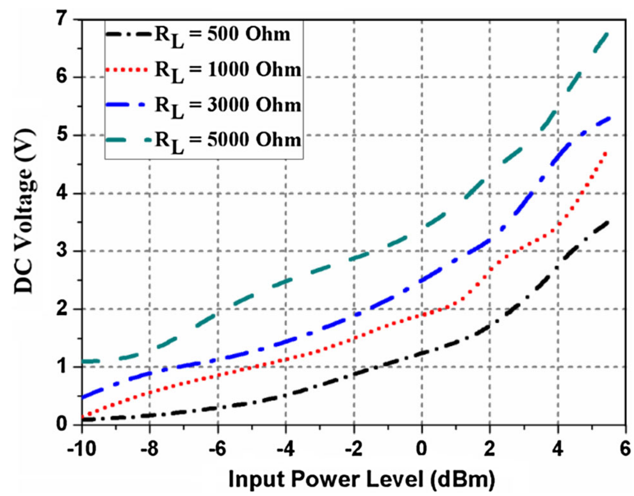

Fig. 12 Output DC voltage at different load resistance

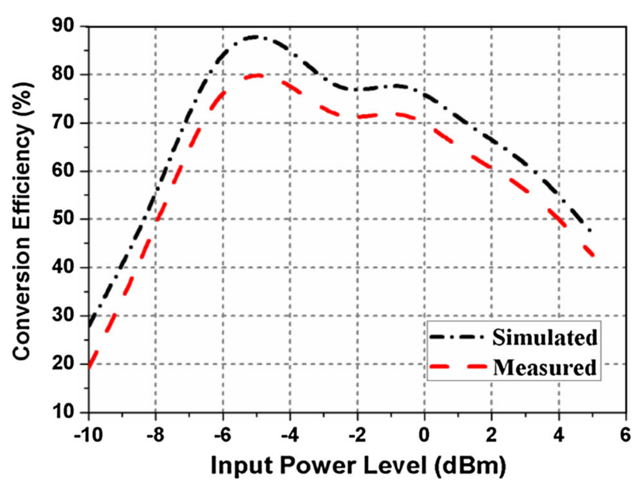

Fig. 13 Simulated and measured conversion efficiency of the rectenna

Table 2 Comparison of proposed work with the reported work

References	Resonating frequency (GHz)	Maximum conversion efficiency (%)	Maximum efficiency at input power (mW)
Yoo and Chang (1992)	24	54	130
Shinohara et al. (2011)	35	52	25.6
Collado and Georgiadis (2013)	25.7	15	6.33
Ladan et al. (2014)	35	39	120
Li and Li (2004)	24	42	18
This Work	24	80	3.16

$$P_r = \left(\frac{\lambda}{4\pi r}\right)^2 P_t G_t G_r \quad (7)$$

$$\eta_{CE}\% = \frac{P_{DC}}{P_{in}} \times 100\% = \frac{V_{DC}^2}{R_L.P_{in}} \times 100\% \quad (8)$$

For the measurement, a high gain Horn antenna is used for transmitting the input power. Figure 12 shows output DC voltage at 24.25 GHz for different values of load resistance and a maximum DC voltage of 6.82 V is obtained at 5 dBm. The maximum conversion efficiency achieved at 5 dBm is 80% as shown in Fig. 13. The rectenna is kept at a distance of 1.5 m for measuring the output voltage.

A comparison of present work with the reported rectenna structures is presented in Table 2. The rectenna designs suggested in the literature are mainly non-planar structures with larger dimensions and low conversion efficiency. This may be due to the degraded performance of the Schottky diode at high frequencies. On the other hand, the proposed rectenna configuration consists of a circularly polarized antenna integrated into the front region of the GFET-based rectifier. The proposed rectenna displays compact size and maximum conversion efficiency of 80%.

4 Conclusion

In this article, a compact wideband rectenna based on graphene FET and monopole antenna is designed. The proposed rectenna is designed to harvest ambient RF energy available in the environment within the frequency range of 22.5–27.5 GHz. From the results, it can be concluded that the proposed rectenna shows a maximum conversion efficiency of 80% at 5 dBm for the load of 5 KΩ. Compared to the other reported rectenna configurations, the proposed rectenna makes use of a GFET-based rectifier and has an output voltage of 6.82 V, hence making it useful for biomedical applications in wearable or implantable devices.

References

A. Collado, A. Georgiadis, 24 GHz substrate integrated waveguide (SIW) rectenna for energy harvesting and wireless power transmission, in: 2013 IEEE MTT-S int. Microwave symp. Dig., pp. 1–3 (2013)

Ansys Corporation, HFSS, suite v15, Pittsburg (PA), USA (2014)

Chandravanshi S, Sarma SS, Akhtar MJ (2018) Design of triple band differential rectenna for RF energy harvesting. IEEE Trans Antennas Propag 66(6):2716–2726

Cui YH, Li RL, Fu HZ (2014) A broadband dual-polarized planar antenna for 2G/3G/LTE base stations. IEEE Trans Antennas Propag 62(9):4836–4840

D. H. Li, K. Li, A novel high-efficiency rectenna for 35 GHz wireless power transmission, in: Proc. 4th Int. Microw. Millimeter-wave Technol. Conf., pp. 114–117 (2004)

Georgiadis A, Andia GV, Collado A (2010) Rectenna design and optimization using reciprocity theory and harmonic balance analysis for electromagnetic (EM) energy harvesting. IEEE Antennas Wirel Propag Lett 9:444–446

Georgiou O, Mimis K, Halls D, Thompson WH, Gibbins D (2016) How many Wi-Fi APs does it take to light a light bulb? IEEE Access 4:3732–3746

Jabbar H, Song YS, Jeong TT (2010) RF energy harvesting system and circuits for charging of mobile devices. IEEE Trans. Cons. Electron. 56(1):247–253

Keysight Technologies, ADS, 2015. http://www.keysight.com/en/pc-1297113/

Ladan S, Guntupalli AB, Wu K (2014) A high-efficiency 24 GHz rectenna development towards millimeter-wave energy harvesting and wireless power transmission. IEEE Trans. Circuits Syst. I Reg. Pap. 61(12):3358–3366

Mimis K, Gibbins D, Dumanli S, Watkins GT (2015) Ambient RF energy harvesting trial in domestic settings. IET Microw. Antennas Propag. 9(5):454–462

Monti G, Congedo F, De Donno D, Tarricone L (2012a) Monopole-based rectenna for microwave energy harvesting of UHF RFID systems. Progress Electromagn. Res. C 31:109–121

Monti G, Corchia L, Tarricone L (2012b) ISM band rectenna using a ring loaded monopole. Progress Electromagn. Res. C 33:1–15

N. Shinohara, K. Nishikawa, T. Seki, K. Hiraga, Development of 24 GHz rectennas for fixed wireless access, in: URSI Gen. Assemb. Sci. Symp., pp. 1–4 (2011)

Okba A, Takacs A, Aubert H, Charlot S, Calmon P-F (2017) Multiband rectenna for microwave applications. C R Phys 18(2):107–117

Schwierz F (2010) Graphene transistors. Nat. Nanotech. 5:487–496

Singh N, Kanaujia BK, Beg MT, Mainuddin, Khan T, Kumar S (2018a) A dual polarized multiband rectenna for RF energy harvesting. AEU-Int. J. Electron. Commun. 93:123–131

Singh N, Kanaujia BK, Beg MT, Mainuddin, Kumar S, Khandelwal MK (2018b) A dual band rectifying antenna for RF energy harvesting. J Comput Electron 17(4):1748–1755

Song C, Huang Y, Zhou J, Zhang J, Yuan S, Carter P (2015) A highefficiency broadband rectenna for ambient wireless energy harvesting. IEEE Trans Antennas Propag 63(8):3486–3495

Sun H, Guo Y-X, He M, Zhong Z (2012) Design of a high efficiency 2.45-GHz rectenna for low-input-power energy harvesting. IEEE Antennas Wirel Propag Lett 11:929–932

Sun H, Guo Y-X, He M, Zhong Z (2013) A dual-band rectenna using broadband Yagi antenna array for ambient RF power harvesting. IEEE Antennas Wirel Propag Lett 12:918–921

Valenta CR, Durgin GD (2014) Harvesting wireless power: survey of energy-harvester conversion efficiency in far-field, wireless power transfer systems. IEEE Microw. Mag. 15(4):108–120

Yang Y, Li J, Li L, Liu Y, Zhang B, Zhu H, Huang K (2018) A 5.8 GHz circularly polarized rectenna with harmonic suppression and rectenna array for wireless power transfer. IEEE Antennas Wirel Propag Lett 17(7):1276–1280

Yoo TW, Chang K (1992) Theoretical and experimental development of 10 and 35 GHz rectennas. IEEE Trans Microw Theory Tech 40(6):1259–1266

Zhang Q, Ou J, Wu Z, Tan H (2018) Novel microwave rectifier optimizing method and its application in rectenna designs. IEEE Access 6:53557–53565